Available online at www.sciencedirect.com
SCIENCE DIRECT
Biochimica et Biophysica Acta 1757 (2006) 273–283
BIOCHIMICA ET BIOPHYSICA ACTA
BBA
http://www.elsevier.com/locate/bba

Spectral and kinetic resolution of the bc_1 complex components in situ: A simple and robust alternative to the traditional difference wavelength approach

Vladimir P. Shinkarev *, Antony R. Crofts, Colin A. Wraight

Department of Biochemistry, University of Illinois at Urbana-Champaign, 156 Davenport Hall, 607 South Mathews Avenue, Urbana, IL 6l80l, USA

Received 26 December 2005; received in revised form 31 March 2006; accepted 1 April 2006
Available online 19 April 2006

Abstract

The kinetics of the cytochrome (cyt) components of the bc_1 complex (ubiquinol: cytochrome *c* oxidoreductase, Complex III) are traditionally followed by using the difference of absorbance changes at two or more different wavelengths. However, this difference-wavelength (DW) approach is of limited accuracy in the separation of absorbance changes of components with overlapping spectral bands. To resolve the kinetics of individual components in *Rhodobacter sphaeroides* chromatophores, we have tested a simplified version of a least squares (LS) analysis, based on measurement at a minimal number of different wavelengths. The success of the simplified LS analysis depended significantly on the wavelengths used in the set. The "traditional" set of 6 wavelengths (542, 551, 561, 566, 569 and 575 nm), normally used in the DW approach to characterize kinetics of cyt c_{tot} (cyt c_1+cyt c_2), cyt b_L, cyt b_H, and P870 in chromatophores, could also be used to determine these components via the simplified LS analysis, with improved resolution of the individual components. However, this set is not sufficient when information about cyts c_1 and c_2 is needed. We identified multiple alternative sets of 5 and 6 wavelengths that could be used to determine the kinetics of all 5 components (P870 and cyts c_1, c_2, b_L, and b_H) simultaneously, with an accuracy comparable to that of the LS analysis based on a full set of wavelengths (1 nm intervals). We conclude that a simplified version of LS deconvolution based on a small number of carefully selected wavelengths provides a robust and significant improvement over the traditional DW approach, since it accounts for spectral interference of the different components, and uses fewer measurements when information about all five individual components is needed. Using the simplified and complete LS analyses, we measured the simultaneous kinetics of all cytochrome components of bc_1 complex in the absence and presence of specific inhibitors and found that they correspond well to those expected from the modified Q-cycle. This is the first study in which the kinetics of all cytochrome and reaction center components of the bc_1 complex functioning in situ have been measured simultaneously, with full deconvolution over an extended time range.

Keywords: bc_1 complex; Electron transfer; Spectral deconvolution; Kinetics; Least squares; *Rhodobacter sphaeroides*

1. Introduction

The cytochrome (cyt) bc_1 complex (ubiquinol: cytochrome *c* oxidoreductase, Complex III) plays a central role in free energy transduction in biomembranes [1–5]. It oxidizes ubiquinol, reduces cytochrome *c*, and generates a transmembrane electrochemical gradient of protons [1–5] that is used to drive ATP synthesis, ion transport, and other kinds of work [2]. The cyt bc_1 complex is a functional dimer, each monomer of which has four redox centers (two hemes in cytochrome *b* (b_L and b_H), cytochrome c_1 and an iron–sulfur protein, ISP) and at least two quinone-binding sites.

The photosynthetic bacterial system has been used for over 30 years as a model system for studying the structure and function of the general class of bc_1-type complexes — for two important and continuing reasons. First, light activation via the reaction center (RC) allows kinetic studies of the cytochrome components in situ, on a time scale unmatched by any respiratory system. Second, the photosynthetic bacterial complex is unusual in having very distinctive spectra for the b_H and b_L hemes, which allows

Abbreviations: CCCP, carbonyl cyanide m-chlorophenylhydrazone; cyt, cytochrome; DW, difference-wavelength; ISP, Rieske iron–sulfur protein; LS, least squares; RC, photosynthetic reaction center; Qi, Qo, quinone reducing and quinol oxidizing sites of bc_1 complex, respectively; b_L and b_H, low- and high-potential hemes of cytochrome *b*, respectively; *Rb.*, *Rhodobacter*; DAD, 2,3,5,6-tetramethyl-p-phenylenediamine

* Corresponding author. Tel.: +1 217 333 8725; fax: +1 217 244 6615.
E-mail address: vshinkar@uiuc.edu (V.P. Shinkarev).

0005-2728/$ - see front matter © 2006 Elsevier B.V. All rights reserved.
doi:10.1016/j.bbabio.2006.04.003

discrimination between these components that is much more difficult and is commonly avoided in other systems, including mitochondria. As a result, purple bacterial chromatophores have become a standard model system for functional studies of the bc_1 complexes. The bc_1 complex from *Rhodobacter sphaeroides* used in these studies is therefore representative of the general class of bc_1-type complexes, and comparative studies have shown that the functional core, which is structurally conserved across the bacterial–mitochondrial divide, is also conserved at the level of basic mechanism.

The kinetics of the cytochrome components of the bc_1 complex and of the RC photopigment, P870, in chromatophores are traditionally followed by using the difference of absorbance changes at two or more wavelengths [6–9]. Such a difference-wavelength (DW) approach has been the de facto method in studies of the bc_1 complex [8]. However, we recently reported that the DW approach can lead to significant errors in the kinetics of cyts c_1 [10], c_2 [10] and b_L [11], especially when the concentration changes of the component of interest are relatively small.

Several approaches have been suggested to restore individual cytochrome components from overlapping spectra (see, e.g., [12–16]). To ensure proper deconvolution of the kinetics of individual components in chromatophores, where significant spectral interference is observed, we have used least squares (LS) analysis [11], based on: (i) measured kinetic traces for 36 wavelengths at 1 nm intervals between 540 and 575 nm, and (ii) newly determined difference spectra of all individual components of cyclic electron transport. While providing the best available accuracy in deconvoluting the individual overlapping components, this approach is impractical for routine experiments because of the large number of measurements required.

In the present work, we have explored a simplified LS analysis, utilizing a minimal number of wavelengths that is very suitable for routine experiments. We found different sets of 5 or 6 wavelengths that could be used to determine simultaneous kinetics of photochemical reaction center, cyts c_1, c_2, b_L, and b_H, with an accuracy comparable to that of LS analysis based on the full set of wavelengths. We conclude that the simplified version of LS deconvolution provides a robust and simple improvement on the traditional DW approach. The LS method automatically takes care of spectral interference of different components, and needs fewer measurements for determination of the kinetics of all individual components. To facilitate application of the simplified LS approach, we determined the coefficients needed for calculating the kinetics of the individual components using simple spreadsheet software. Using the simplified LS analysis, we measured simultaneous kinetics of all 5 components of the photosynthetic chain, including the three heme centers of the bc_1 complex, in the absence and presence of specific inhibitors.

2. Materials and methods

2.1. Growth of cells and isolation of chromatophores

Cells of *Rhodobacter sphaeroides* Ga (a strain with a reduced complement of carotenoids, but otherwise wild type photosynthetic apparatus) were grown photosynthetically at 30 °C in Sistrom's medium. After cell breakage, chromatophores were isolated by differential centrifugation [17].

2.2. Spectrophotometric measurements

Flash-induced kinetics of cytochromes, P870, and the electrochromic carotenoid bandshift were measured with a single beam kinetic spectrophotometer of local design. Excitation of photochemical reaction centers was provided by a xenon flash (~ 5 μs half-width), with complementary filters to minimize cross talk between actinic and measuring beams. The monochromator was calibrated using Hg-vapor lamp emission bands in the α-band region. Slit widths were set so as to give a spectral bandwidth of 1.8 nm.

The electrogenic activity of the photosynthetic chain was monitored at 503 nm through the carotenoid electrochromic bandshift. Contributions of electrochromic changes to kinetics of redox centers were minimized by including 25 μM CCCP and 5 μM gramicidin to catalyze rapid dissipation of the proton gradient.

2.3. Least squares method

The least squares (LS) method minimizes the sum of the squares of the deviations of experimentally measured values of absorbance changes from a theoretical expectation (see, e.g., [13,15,16,18,19]). The LS method is based on the representation of absorbance changes at each wavelength λ_i (i=1,..., L), as the sum of the absorbance changes of each individual component j, j=1,...,N, present in the system:

$$A(\lambda_i) = \sum_{j=1}^{N} A_j(\lambda_i) \tag{1}$$

in turn, it is assumed that absorbance of each j-th component obeys the Beer–Lambert Law, i.e., the optical density of unit path length is the product of the millimolar extinction coefficient s_j (with units of mM^{-1} cm^{-1}) at each wavelength and the concentration c_j (in mM) of each component in solution:

$$A_j(\lambda_i) = s_j(\lambda_i)c_j \tag{2}$$

Combining Eqs. (1) and (2) we have:

$$A(\lambda_i, t_k) = \sum_{j}^{N} s_j(\lambda_i)c_j(t_k) \tag{3}$$

We assumed that only the concentrations of individual components depend on time, c_j=$c_j(t_k)$, k=1,..., M. In matrix notation, this can be presented as follows:

$$A = SC \tag{4}$$

where $A = \{a_{ik}\} \equiv A(\lambda_i,t_k),(i = 1,\ldots,L; k = 1,\ldots,M)$; $S = \{s_{ij}\} \equiv s_j(\lambda_i),(i = 1,\ldots,L; j=1,\ldots,N);(j=1,\ldots, k=1,\ldots,M)$. The matrix

$$\bar{C} = (S^T S)^{-1} S^T A \tag{5}$$

where superscript 'T' indicates the transpose of a matrix, gives the best estimate of unknown matrix C from known matrix S and measured matrix A [19–22]. Solution (5) is valid only when square matrix S^TS is invertible (nonsingular). This is the case if the number of wavelengths is greater than the number of individual components, and no one component's spectrum can be expressed as a linear combination of the other components.

The accuracy of deconvolution was checked by inspecting residuals $A-S\bar{C}$. Additionally, we estimated the condition number of the matrix $(S^TS)^{-1}$ S^T in Eq. (5) [23–26], (defined as a product of norms of original and inverse matrices), which is calculated here as the ratio of the largest and smallest singular values of the matrix. When the condition number is large, small changes in the absorbance differences can lead to large relative changes of the components of the matrix $\bar{C}$.

All calculations were performed using Matlab software (The Mathworks, Inc.).

2.4. Reagents

Antimycin A, gramicidin, myxothiazol, stigmatellin, DAD, PMS, CCCP, and Tris were obtained from Sigma-Aldrich (St. Louis, MO). Inhibitors and uncouplers were dissolved in ethanol and stored at −20 °C.

3. Results

In the traditional DW analysis, the redox state changes of individual carriers are measured using the difference of absorbance at two or more wavelengths. Much previous work has been based on a set of 6 wavelengths, intended to separate the 4 components P870, "cyt c_{tot}", cyt b_H, cyt b_L, where cyt c_{tot} is the sum of cyt c_1 and cyt c_2 [1,8,27]. However, when knowledge of kinetics of all these components is needed, i.e., including cyts c_1 and c_2 separately, the number of wavelengths used for their measurements increases significantly, to at least 9. Since a significant amount of data using these wavelength sets resides in the literature, we first attempt to use the "traditional" set of 6 wavelengths to obtain a self-consistent LS solution. Using the same sets of wavelengths has two-fold advantage: (i) it gives the opportunity of direct comparison between LS and DW approaches; (ii) it allows recalculating, if needed, previously obtained data for wild type and mutant chromatophores. Initially, we consider the application of the simplified LS analysis for determination of four individual components, P870, cyt c_{tot}, cyt b_H and cyt b_L. Later, we will extend this analysis to determine the separate kinetics of cyts c_1 and c_2 as well.

3.1. Determination of P870, cyt c_{tot}, cyt b_H and cyt b_L using the traditional set of 6 wavelengths

To simultaneously characterize 4 unknown components (P870, cyt c_{tot}, cyt b_H and cyt b_L) the traditional DW approach employs 6 wavelengths: 551–542 nm for cyt c_{tot} (cyt c_1 plus cyt c_2) [6,7], 561–569 nm for cyt b_H [8], 566–575 nm, minus 1/2 of 561–569 nm for cyt b_L [9], and 542 nm for P870 [28]. In general, 4 appropriately chosen wavelengths can suffice to recover the kinetics of 4 spectrally distinct components (assuming there are no other components with significant absorbance). Measurements at 6 wavelengths could decrease errors in the determination of their kinetics, but the overall noise level will depend on the quality of the additional traces.

3.1.1. LS analysis based on traditional set of wavelengths

Fig. 2 shows the flash-induced kinetics of the 4 individual components determined by LS analysis from the kinetics of the absorbance changes measured at different wavelengths, including the traditional set of 6 ("gray": 542, 551,561, 566, 569 and 575 nm), a subset of 4 ("black": 542, 551, 561, and 566 nm), and 36 ("light gray": from 540 to 575 with 1 nm step intervals) different wavelengths. One can see that the kinetics of individual components were similar but not identical for these sets of wavelengths. The set of 6 wavelengths (542, 551, 561, 566, 569 and 575 nm) reproduces the kinetics of all 4 individual components with reasonable noise level. In some cases the gray and light gray traces overlap so completely that they are only distinguished by their noise levels. The set of 4 wavelengths (542, 551, 561, and 566 nm) was insufficient to properly reproduce the kinetics of all electron carriers (see Fig. 2B for cyt *c*). The set of 5 wavelengths (542, 551, 561, 566, and 569 nm; not shown) better reproduces the kinetics of cyt c_{tot}, but has significantly increased noise level (not shown, but see Fig. 4B below).

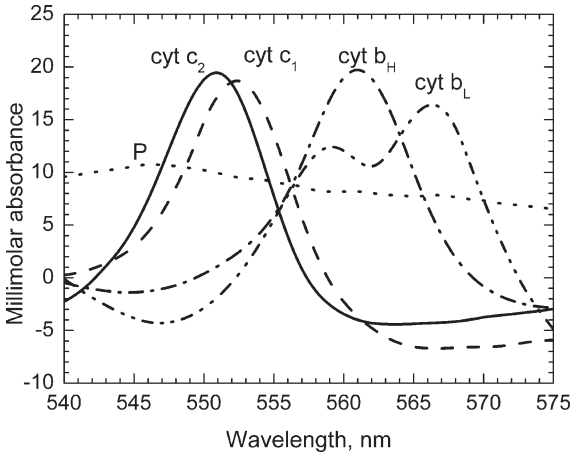

Fig. 1. Difference spectra of individual components in the 540–575 nm region in *Rb. sphaeroides* chromatophores used in this paper for the deconvolution [7,9,11].

We have shown previously that there are some significant differences between the DW approach and LS analysis based on the full set of 36 wavelengths. These differences apply equally well to comparison with the smaller sets used here, but were fully discussed previously [10,11] and will only be considered briefly in Section 4.

3.1.2. Error analysis of LS deconvolution based on the traditional set of wavelengths

The quality of deconvolution shown in Fig. 2 can be estimated by calculating the difference between the original and fitted transients at each wavelength, i.e., residuals. Fig. 3 shows flash-induced absorption changes at four (panel A) and six (panel B) different wavelengths together with the respective residuals (shown in gray), based on deconvolution of 4 or 6 "traditional" wavelengths, respectively. The small level of residuals for the set of 6 wavelengths indicates that the spectra used in the deconvolution could be fitted well to the observed absorption changes. However, in the case of 4 wavelengths, there are significant residuals at each wavelength, but especially at 551 nm, due to the artificial nature of cyt c_{tot} ($=c_1+c_2$) and the inability to deconvolute the kinetics of cyts c_1 and c_2 accurately in order to generate the cyt c_{tot} kinetics.

Additional insight into the sensitivity of deconvolution to errors of measurements at individual wavelengths can be gained from the noise level of the resolved components, determined for different sets of wavelengths used for deconvolution (Fig. 4). To do this we input random noise of the same amplitude at each wavelength used for the LS analysis, based on the spectra shown in Fig. 1.

Fig. 4 shows that the errors of deconvolution of individual components depend significantly on the set of wavelengths used. The lowest error is observed when all 36 wavelengths are

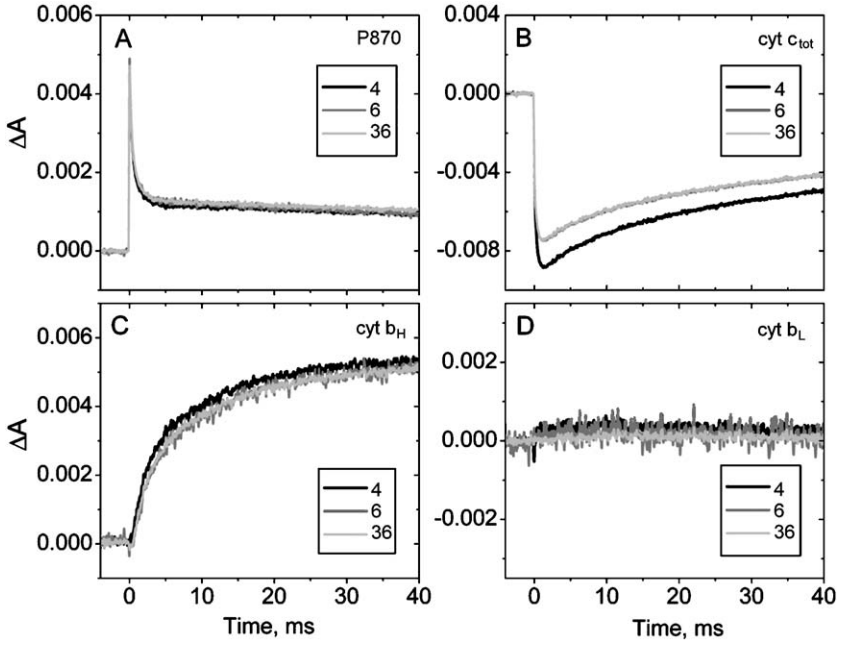

Fig. 2. Flash-induced kinetics of $P870^+$, cyt c_{tot}, cyt *b*H, and cyt *b*L in *Rb. sphaeroides* chromatophores in the presence of antimycin. The kinetics were determined by LS analysis from the kinetics of absorbance changes measured at different sets of wavelengths, including sets of 4 ("black": 542, 551, 561, and 566 nm), 6 ("gray": 542, 551, 561, 566, 569 and 575 nm), and 36 ("light gray": from 540 to 575 with 1 nm step) different wavelengths. Chromatophores were suspended in 50 mM Tris–HCl buffer (pH 7.4) with 10 mM potassium ferrocyanide, 100 μM DAD, 2 mM NaCN, 25 μM CCCP, 5 μM gramicidin, 5 μM antimycin A. Kinetic traces at each wavelength are the average of 2 traces, with 30 s between measurements and were recorded with an instrument response time of 70 μs. The redox potential was ≈280 mV.

taken into account (Fig. 4E). The noise is higher when only 4 wavelengths in the set are used (Fig. 4A). Adding 569 nm to the set substantially increases the noise level for b_L and b_H hemes (Fig. 4B) because this wavelength does not distinguish strongly between P870 and cyt b_L and between cyts c_1 and b_H. It therefore acts primarily as a source of noise. However, a second subset of 5 of the "traditional" wavelengths (Fig. 4C) does not increase the noise of the deconvolution, and the set of 6 wavelengths (Fig. 4D) suppresses the extra noise introduced by 569 nm alone.

Due to the linear nature of Eq. (5), the error in determining each component is proportional to the errors in determining absorbance at each wavelength. For each set of wavelengths, one can calculate the ratio of the standard deviation of the determination of each individual component to the standard deviation of the absorbance measurement (assuming that it is the same at each wavelength). Knowledge of this ratio would allow an investigator to determine the accuracy of the absorbance measurement required to reach a given signal to noise ratio and to choose an appropriate set of wavelengths needed for use in a simplified LS analysis.

3.1.3. Kinetics of cyt c_1 and c_2 cannot be recovered from the "traditional" wavelength set

Figs. 2–4 indicate that the simplified LS deconvolution based on the "traditional" set of 6 wavelengths (542, 551, 561, 566, 569, and 575 nm) can be used to simultaneously characterize cyt c_{tot} ($=c_1+c_2$), P870, cyt b_H and cyt b_L in *Rb. sphaeroides* chromatophores. However, our attempts to use these wavelengths to extract the kinetics of cyts c_1 and c_2, separately, were completely unsuccessful (not shown, but see Fig. 8H below). The failure of determining the kinetics of 5 individual components from measurements at 6 different wavelengths clearly indicates that not only the number of wavelengths employed, but also, the choice of wavelengths is important for proper LS deconvolution.

Meinhardt and Crofts [7] suggested measuring the kinetics of cyt c_2 at 550–554 nm and cyt c_1 at 552–548 nm. Thus, to determine the kinetics of all 5 individual components in *Rb. sphaeroides* chromatophores (P870, cyts c_1, c_2, b_H, and b_L) using the DW approach, one needs to measure kinetics of absorbance changes at 9 different wavelengths. In the next section, we investigate the possibility of reducing the number of wavelengths needed to determine the kinetics of all individual components in chromatophores using simplified LS analysis.

3.2. New minimal sets of wavelengths needed to characterize 5 unknown components (P870, cyt c_1, cyt c_2, cyt b_H and cyt b_L)

Our noise analysis (Fig. 4) clearly indicates that the quality of LS deconvolution significantly depends on the choice of wavelengths used for the deconvolution. This is expected because only particular wavelengths exhibit distinct differences in the spectra of individual components presented in Fig. 1.

3.2.1. Wavelengths suited for LS deconvolution of 5 individual components

There are many different ways to choose wavelengths for deconvolution. For example, one can choose wavelengths corresponding to the maxima in the original difference spectra,

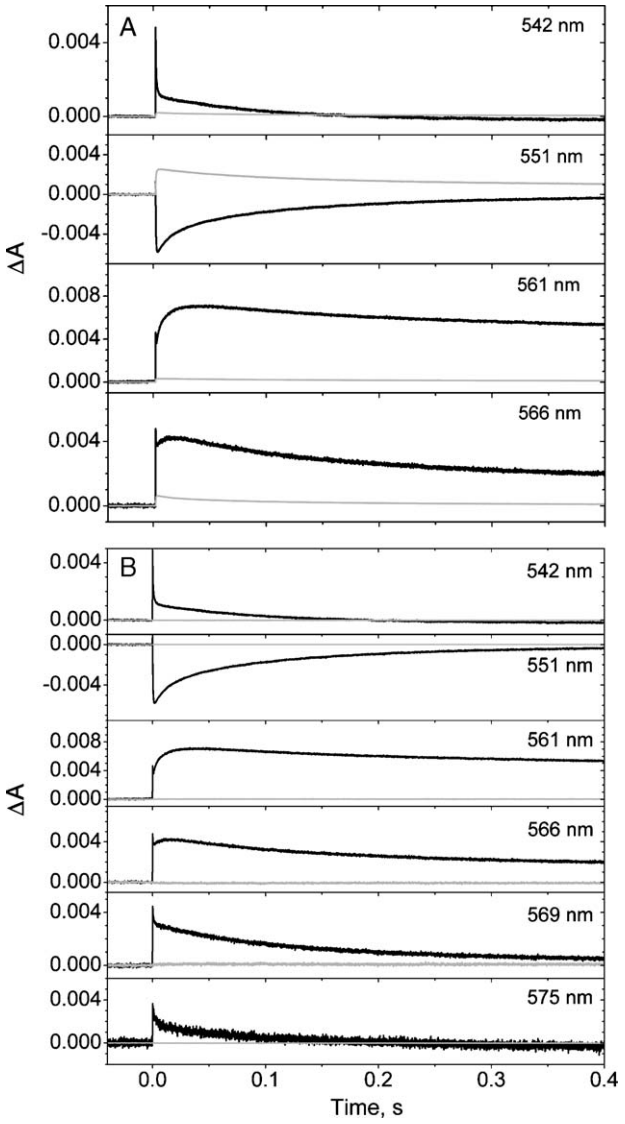

Fig. 3. Flash-induced absorption changes at four (A) and six (B) different wavelengths. Also shown are the residuals (gray). Conditions as in Fig. 2.

or wavelengths corresponding to maximal differences between difference spectra of individual electron carriers. A more formal approach is to choose wavelengths in the set by minimizing the condition number of the matrix of Eq. (5) (defined as a product of norms of original and inverse matrices), responsible for the upper estimate of error propagation [25]. For a given number of wavelengths, n, the condition number indicates the quality of the deconvolution. Fig. 5 shows the 10 smallest values of condition numbers for different sets of 5, 6 and 7 wavelengths, with integral wavelength values. One can draw the conclusion that there are many different sets of wavelengths that give similarly small values of the condition number, and all can be used for deconvolution with similar errors. However, there are many other sets of wavelengths for which the condition numbers are large (some $>10^3$); the sets with large condition number are useless for the LS deconvolution.

For sets of 5 wavelengths, the lowest condition number ($k=4.69$) was observed for 540, 548, 555, 563 and 568 nm. The set of 5 "traditional" wavelengths, 542, 551, 561, 566 and 569 gave condition number $k=47.3$. This large condition number reflects the substantially greater noise level seen for this set (Fig. 4B).

The lowest condition number, $k=4.55$, for the set of 6 wavelengths was observed for 540, 548, 555, 563, 569, and 575 nm. The set of "traditional" wavelengths, 542, 551, 561, 566, 569, and 575 nm gives condition number $k=15.03$. This relatively large value accounts for the inability to recover the separate kinetics of cyts c_1 and c_2 from this set.

Sets with 6 wavelengths had the lowest condition numbers, $k<4.7$, while the lowest values for sets of 7 wavelengths were rather invariant around $k=5.15$. The non-monotonic dependence of lowest condition number on the number of wavelengths in the set arises from two opposing trends. Increasing the number of wavelengths in the set should generally decrease the condition number, because it effectively increases the number of repetitions (averaging). On the other hand, if an added wavelength does not improve the separation of individual components, the condition number increases.

3.2.2. Kinetics of cyts c_1, c_2, and c_{tot} determined by the simplified LS deconvolution based on small sets

The signal to noise ratio for the deconvolution of cyts c_1 and c_2 was improved significantly by wavelength sets with low condition number. Fig. 6 shows flash-induced kinetics of cyts c_{tot}, c_1 and c_2, determined by LS analysis from the kinetics of absorbance changes measured with different sets of wavelengths.

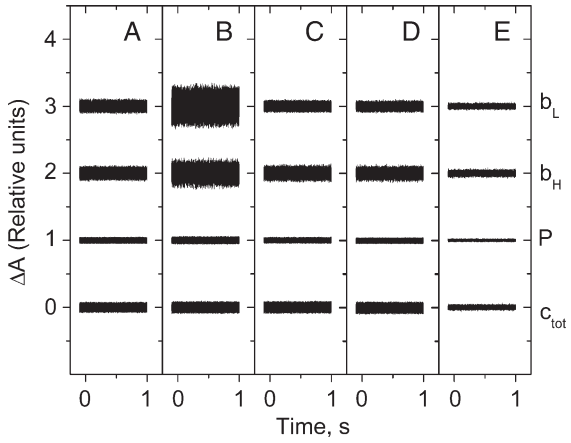

Fig. 4. Noise levels in the kinetics of cyt c_{tot}, $P870^+$, cyt bH, and cyt bL determined by LS analysis, using the traditional wavelength set or subsets. Random noise generated with uniform distribution on the interval (−0.05, 0.05) was applied to each of the following wavelengths used for the LS analysis: 542, 551, 561 and 566 nm in panel A (4 wavelengths), 542, 551, 561, 566 and 569 nm in the panel B (5 wavelengths), 542, 551, 561, 566, and 575 nm in panel C (5 wavelengths), 542, 551, 561, 566, 569 and 575 nm in panel D (6 wavelengths), and 36 wavelengths from 540 to 575 nm with 1 nm step in panel E. Curves are shifted vertically to improve visibility. The standard deviation in the measurement of cyt c_{tot}, $P870^+$, cyt bH, and cyt bL is equal to that of the absorption measurements (assuming that the standard deviation of the absorption changes is the same for each wavelength) multiplied by 1.16, 0.88, 1.55, and 1.49 in panel A, 1.33, 0.85, 2.73, and 4.42 in panel B, 1.34, 0.80, 1.66, and 1.31 in panel C, 1.33, 0.78, 1.54, and 1.22 in panel D and 0.55, 0.29, 0.73, and 0.62 in panel E, respectively.

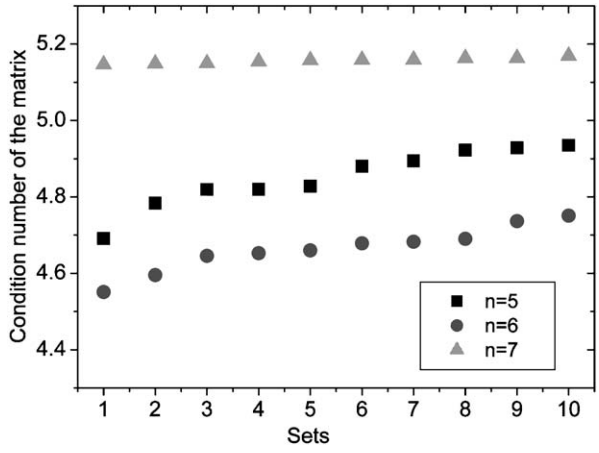

Fig. 5. The 10 smallest condition numbers of matrix $(S^T S)^{-1}S$ for data sets including 5, 6, and 7 wavelengths. The set 540, 548, 555, 563 and 568 nm has lowest condition number (k=4.69) of all sets with 5 wavelengths. The set 540, 548, 555, 563, 569, and 575 nm has lowest condition number (k=4.55) from all sets with 6 wavelengths. The set 540, 549, 554 556, 563, 566, and 570 nm has lowest condition number (k=5.15) from all sets with 7 wavelengths.

These sets include one or two additional wavelengths, corresponding closely to the largest differences in the cyts c_1 and c_2 difference spectra. These new sets of wavelengths (panels A–E) gave good descriptions of the c-type cytochromes, comparable to those determined using the full set of wavelengths (panel F). Only in panel D (with k=12.66) are the relative amplitudes of cyt c_1 and c_2 substantially different from those in panel F.

For all the traces shown, the kinetics of cyt c_1 are slower than those of cyt c_2. Our deconvolution supports the conclusion of Meinhardt and Crofts [7] that the fast component of cyt c_{tot} oxidation (at <50 μs) is contributed almost entirely by cyt c_2, while the slow component mostly comes from cyt c_1. The kinetics of cyt c_1 have a delay ~50 μs, which reflects all processes leading to the oxidation of cyt c_1 after P870 photooxidation [10].

The higher noise observed in panel E is mostly due to the presence in the deconvolution of the noisy kinetics of absorbance changes at 575 nm, originating from the lower light intensity due to high absorption of the complementary optical filters used to block the actinic light.

3.2.3. Kinetics of P870 and cyts b_H, and b_L, determined by LS deconvolution with small wavelength sets

Fig. 7 shows the flash-induced kinetics of P870, cyts b_H and b_L in *Rb. sphaeroides* chromatophores determined for the same wavelength sets as in Fig. 6. As before, these sets of wavelengths (panels A–E) gave excellent correspondence of the kinetics of the P870 and *b* hemes with those determined using the full set of 36 wavelengths (panel F). However, the noise level for some deconvolutions is larger than for others (compare heme b_H kinetics in panels A and B).

3.2.4. Error analysis of the LS deconvolution based on new, minimal sets of wavelengths

Many different types of errors can affect the final LS deconvolution. These include errors in measurement of the kinetics of

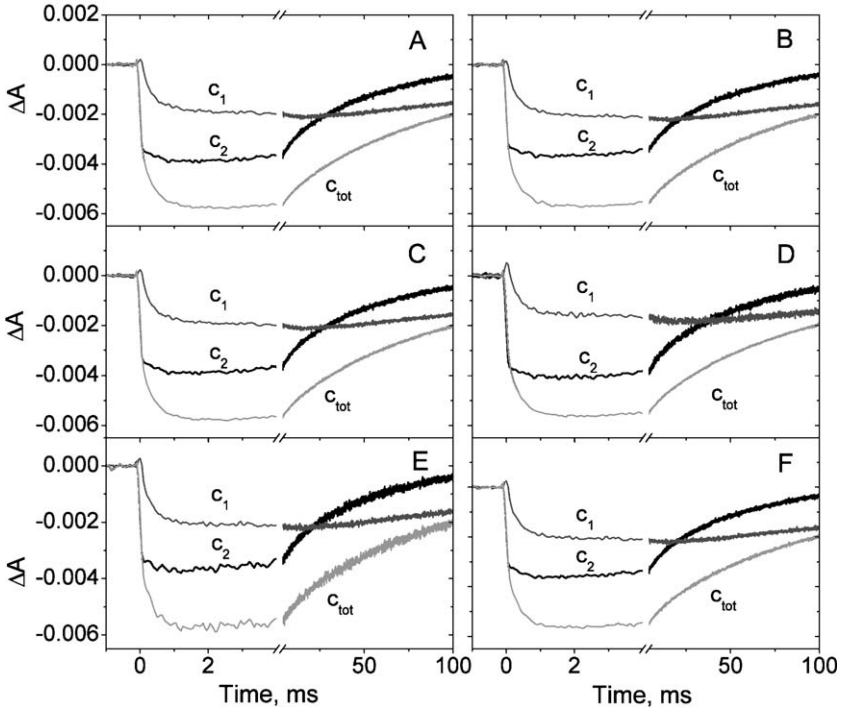

Fig. 6. Flash-induced kinetics of cyts c_{tot}, c_1 and c_2, determined by LS analysis from the kinetics of absorbance changes measured at different sets of wavelength, including 5 (A: 542, 548, 554, 561, 566), (B: 540, 548, 555, 563, 568), 6 (C: 542, 548, 554, 561, 566, 569), (D: 542, 548, 551, 561, 566, 569), (E: 540, 548, 555, 563, 569, 575) and 36 (F: from 540 to 575) different wavelengths. Condition numbers are 6.01 for set A, 4.69 for set B, 6.42 for set C, 12.66 for set D, 4.55 for set E, and 6.82 for set F. Chromatophores were suspended in 50 mM Tris–HCl buffer (pH 7.4) with 3 mM potassium ferrocyanide, 100 μM DAD, 2 mM NaCN, 25 μM CCCP, 5 μM gramicidin, 5 μM antimycin A. Kinetic traces at each wavelength are the average of 4 traces, with 15 s between measurements and were recorded with an instrument response time of 70 μs. The redox potential was 280±30 mV.

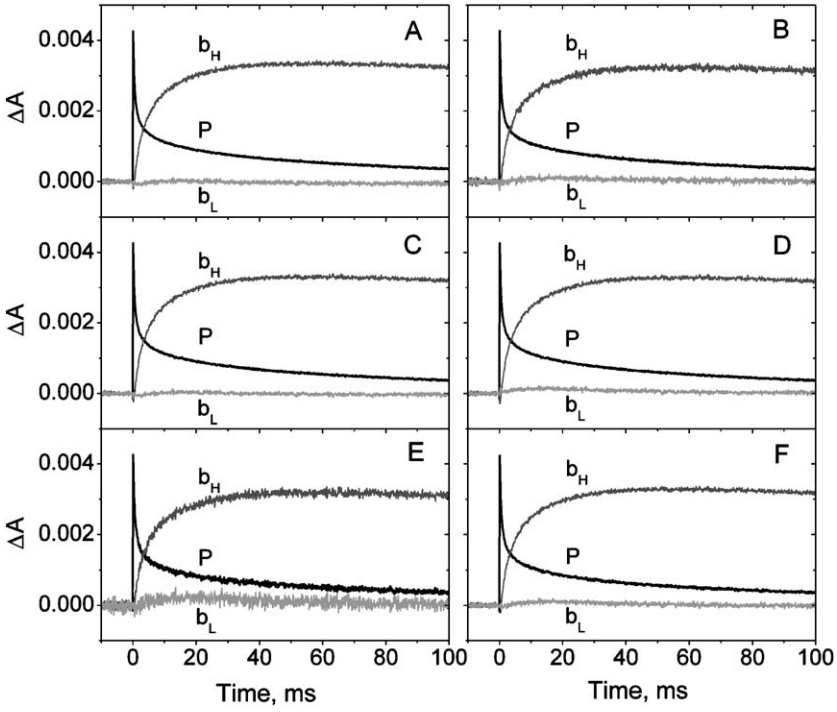

Fig. 7. Flash-induced kinetics of P870, cyts *b*H, and *b*L, determined by LS analysis from the kinetics of absorbance changes measured at different sets of wavelength used in Fig. 6, including 5 (A: 542, 548, 554, 561, 566), (B: 540, 548, 555, 563, 568), 6 (C: 542, 548, 554, 561, 566, 569), (D: 542, 548, 551, 561, 566, 569), (E: 540, 548, 555, 563, 569, 575) and 36 (F: from 540 to 575) different wavelengths. Conditions are as in Fig. 6.

absorbance changes at different wavelengths (signal to noise ratio, spectral resolution and wavelength calibration), errors in the reference spectra of individual components (e.g., Fig. 1), as well as errors originating from inability to distinguish between spectra of individual components (the matrices used in LS analysis could be ill-conditioned, meaning that small changes in the elements of the coefficient matrix cause large changes in the solution). The latter can be estimated by calculating the condition number. It also can be estimated by applying random noise at each wavelength of the set and analyzing the noise appearing in each individual component during LS deconvolution.

Fig. 8 shows the noise originating in all individual components after LS deconvolution, using different sets of wavelengths. At each wavelength of a set, we generated random noise on the interval (−0.1, 0.1), which was used as the input for the deconvolution. One can see that the error (noise) depends significantly on the set of wavelengths used. The smallest errors were observed for 30 and 36 different wavelengths (Fig. 8K, L). However, even in this case, one can see the extra noise in cyts c_1 and c_2, reflecting their spectral similarity The noise level in cyts c_1 and c_2 is larger for smaller sets of wavelengths. For example, for the classic set of wavelengths (previously used to obtain the kinetics of c_{tot}, cyt b_H, cyt b_L and P870) the noise obliterates the kinetics of cyts c_1 and c_2, even though the other components are resolvable (Fig. 8H). This is due to the ill-conditioned nature of the matrix based on this set of wavelengths. All sets for which we were able to recover the kinetics of cyt c_1 and cyt c_2 have additional wavelengths, closely corresponding to the maximum differences between the difference spectra of cyts c_1 and c_2, which are at 548 and 555 nm. There are many "minimal" sets of 5 wavelengths that allow deconvolution of the kinetics of all 5 components, i.e., successfully separating cyts c_1 and c_2 (Fig. 8B–D). Many other sets of wavelengths also give comparable errors of deconvolution of individual components, some of which are shown in Fig. 8.

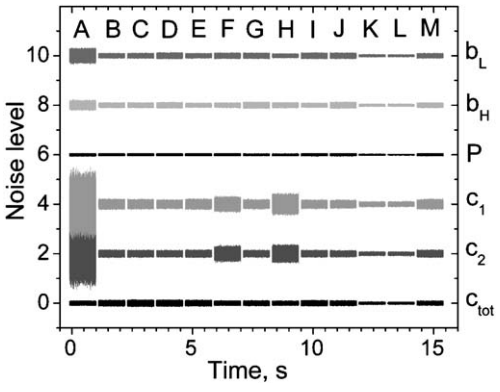

Fig. 8. Noise levels (relative units) in the kinetics of cyt c_2, cyt c_1, $P870^+$, cyt *b*H, and cyt *b*L determined by LS analysis. The random noise generated from uniform distribution on the interval (−0.1, 0.1) was applied to each wavelength of the set. Set A: 542, 551, 561, 566, and 569 nm (condition number, k=47.30); Set B: 542, 548, 554, 561, and 566 nm (k=6.01); Set C: 542, 548, 555, 561, and 566 nm (k=5.74); Set D: 540, 548, 555, 563, and 568 nm (k=4.69); Set E: 542, 548, 554, 561, 566, and 569 nm (κ=6.42); Set F: 542, 548, 551, 561, 566, and 569 nm (k=12.66); Set G: 540, 548, 555, 563, 569, and 575 nm (k=4.55); Set H: 542, 551, 561, 566, 569, and 575 nm (k=15.03); Set I: 540, 549, 555, 562, 568, and 570 nm (k=4.94); Set J: 540, 549, 554, 556, 563, 566, and 570 nm (k=5.15); Set K: 30 wavelengths from 540 to 569 nm (k=6.74); Set L: 36 wavelengths from 540 to 575 nm (k=6.82); Set M: 542, 548, 551, 554, 561, and 566 nm (k=7.57); curves are shifted vertically for better visibility.

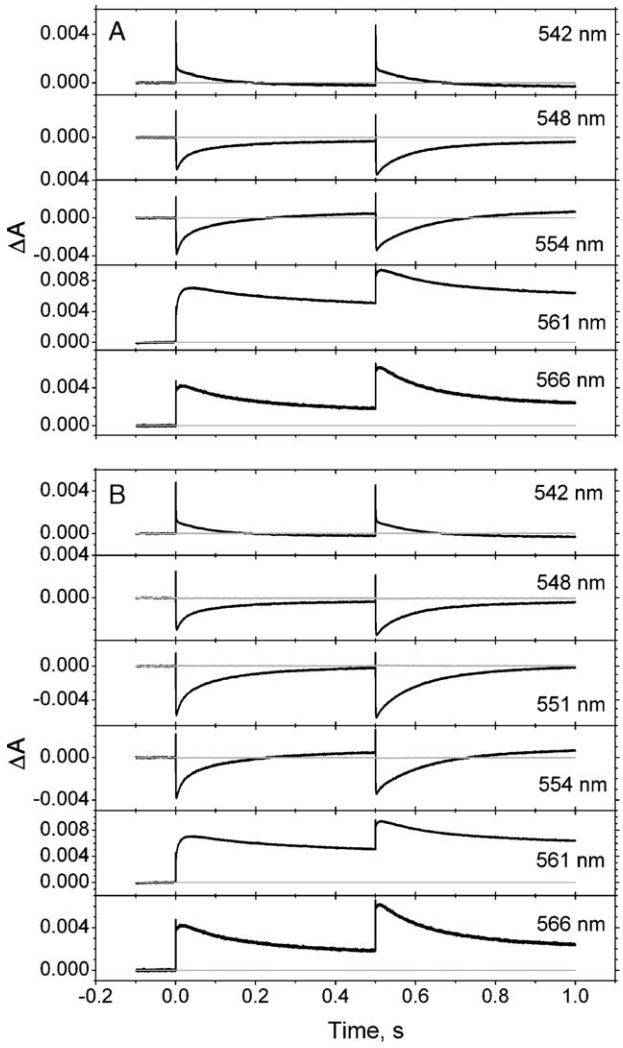

Fig. 9. Flash-induced absorption changes at five (542, 548, 554, 561, and 566 nm; set B in Fig. 8) and six (542, 548, 551, 554, 561, and 566 nm; set M in Fig. 8) different wavelengths together with the differences between measured and predicted changes (shown at the zero level of each curve). Conditions are as in Fig. 2.

Altogether, Fig. 8 indicates that for all analyzed data sets the spectral deconvolution of cyts c_1 and c_2 has the largest uncertainty and the noise level in determination of c_{tot} is always less than the noise levels in cyts c_1 and c_2. Fig. 8 also indicates that the noise in individual components can be larger even when condition number is smaller. For example, the condition number in the panel D (k=4.69) is smaller than that in the panel E (k=6.42). Nevertheless, the noise level in cyts b_L and b_H in panel E is smaller than in the panel D. This is due to the fact that condition number reflects the quality of the deconvolution in terms of the worst-case component. Thus, the larger value of the condition number in the panel E is due to the greater sensitivity of the cyt c_1 deconvolution, not cyt b_L, to the perturbations.

Fig. 9 shows flash-induced absorption changes at five and six different wavelengths together with the differences between measured and deconvolved changes for each individual wavelength. The small magnitude of these differences indicates that the spectra used in the deconvolution can be fitted well to the observed absorption changes. Only two typical examples are shown, but we conclude that several sets of 5 and 6 carefully chosen wavelengths can be used successfully for the LS deconvolution.

4. Discussion

4.1. LS analysis based on small sets of wavelengths is superior to the traditional DW approach

Recently, we compared the kinetics of individual components determined by the traditional DW approach with the results of LS deconvolution [10,11], and found that in certain cases the DW approach was unreliable in extracting accurate kinetic traces for individual components. This failure originates from the inability of the DW method to deal with spectral interference of different components, and it is especially at risk in the separation of the kinetics of cyts c_1 and c_2, and resolution of the kinetics of cyt b_L.

In our original approach [11], we used LS analysis based on the kinetic traces for 36 wavelengths equally spaced over the range between 540 and 575 nm. While providing a high degree of accuracy (partially because of the large number of measurements), this approach demands significant time, making the analysis impractical for routine experiments.

Here, we considered a simplified LS approach based on smaller sets of wavelengths. The LS method inherently takes into account the spectral interference between different components, but it also allows a substantial decrease in the number of wavelengths needed for kinetic measurements (minimally 5 in LS analysis versus 9 in the DW method). Notably, the quality of this simplified LS approach is similar to that for the LS analysis based on the full set of 36 wavelengths. Such simplified LS analysis allows recovery of all the main components of the cyclic electron transport in chromatophores from a minimal number of wavelengths. It is at least as simple as the traditional DW approach, is accurate and highly robust, and can be performed using simple spreadsheet software (see Section 4.3 below). Thus, the simplified LS analysis provides a substantial improvement on the traditional DW method.

4.2. Coefficients for calculating the kinetics of 4 individual components for traditional set of wavelengths

Because of the difficulty of separating the two c-type cytochromes, a substantial amount of work in the literature refers only to 4 components, with cyt c_1+cyt c_2 combined as cyt c_{tot}. Therefore, we briefly consider the impact of LS analysis on the kinetic resolution of these 4 components, with special attention to set of 6 traditional wavelengths used in most previous DW work. The more complete case of 5 components is considered in Section 4.3 below.

Once a set of wavelengths for LS analysis has been specified, one can calculate coefficients needed to describe the kinetics of individual components in situ from the kinetics measured at each wavelength of the set. These coefficients already take into

Table 1
Coefficients needed to restore the concentrations (mM) of individual components in *Rb. sphaeroides* chromatophores from measurements of absorbance changes at 6 "traditional" wavelengths

	542	551	561	566	569	575
Cyt c_{tot}	−0.88	0.98	−0.14	0.08	−0.03	0.01
P870	0.76	0.05	0.04	0.03	0.12	0.07
Cyt b_H	−0.71	0.14	1.13	−0.37	−0.47	0.47
Cyt b_L	0.01	0.02	−0.32	0.68	0.36	−0.89

account the spectral interference of all components included in the analysis. It is clear that to determine the kinetics of four components (P870, cyt c_{tot}, cyt b_L and cyt b_H) the number of the wavelengths in the set should be at least 4. However, we found that the kinetics of individual components determined from a subset of 4 "traditional" wavelengths deviate significantly from curves obtained with more complete LS analysis at 36 wavelengths.

Table 1 gives the coefficients to be used to determine the kinetics of the individual components ($P870^+$, cyt c_{tot}, cyt b_H, and cyt b_L) in chromatophores using the 6 "traditional" wavelengths. With this set, the results of LS deconvolution can be compared directly with the traditional DW approach for the same data sets. The values in Table 1 depend only on the static spectra of the individual components shown in Fig. 1 and do not depend on the flash-induced kinetics of measured absorbance changes. These coefficients can be used to determine the time dependence of individual components. For example, the concentration of $P870^+$ at time τ can be restored from individual traces measured at these wavelengths at time τ as follows:

$$\begin{aligned} Cyt\ c_{tot}(\tau) = &-0.88\Delta A_{542}(\tau) \\ &+ 0.98\Delta A_{551}(\tau) - 0.14\Delta A_{561}(\tau) \\ &+ 0.08\Delta A_{566}(\tau) - 0.03\Delta A_{569}(\tau) \\ &+ 0.01\Delta A_{575}(\tau) \end{aligned} \quad (6)$$

The coefficients in Table 1 allow re-evaluation of existing data taken at these wavelengths, taking into account the spectral interference of individual components. Comparing the results based on DW and LS analyses can provide insight into the effect of spectral interference. The coefficients also can be used to characterize individual components of the bc_1 complex using data sets for chromatophores obtained previously from wild type and mutant cells, as long as the latter do not involve changes in reference spectra.

Table 2
Coefficients for 5 different wavelengths (panel C in Fig. 8), needed to restore the concentrations (mM) of individual components in *Rb. sphaeroides* chromatophores

	542	548	555	561	566
Cyt c_1	0.29	−0.97	1.65	−0.39	−0.57
Cyt c_2	−1.65	1.92	−0.99	0.13	0.54
P870	0.86	0.05	−0.03	0.03	0.12
Cyt b_H	−0.49	0.17	−0.10	1.24	−0.78
Cyt b_L	−0.76	−0.04	0.47	−0.48	0.99

Table 3
Coefficients for 6 different wavelengths (panel I in Fig. 8) needed to restore the concentration (in mM) of individual components in *Rb. sphaeroides* chromatophores, calculated from spectra of individual components

	540	549	555	562	568	570
Cyt c_1	0.43	−0.80	1.56	−0.55	−0.27	−0.49
Cyt c_2	−1.43	1.52	−1.03	0.29	0.53	0.14
P870	0.73	0.16	−0.05	0.07	−0.09	0.28
Cyt b_H	−0.13	0.10	−0.16	1.16	−0.63	−0.38
Cyt b_L	−1.01	−0.18	0.66	−0.33	1.06	0.03

4.3. Coefficients for determining the kinetics of all 5 individual components with new wavelength sets

Our attempts to use only the "traditional" (542, 551, 561, 566, 569, and 575 nm) wavelengths (see above) for extracting kinetics of cyts c_1 and c_2 using simplified LS analysis were unsuccessful (see panel H in Fig. 8). However, the deconvolution of cyts c_1 and c_2 was improved significantly with new sets that included one or two wavelengths, corresponding to the largest differences in the cyts c_1 and c_2 spectra (548 and 555 nm). The best additional wavelengths were found by estimating the condition numbers (Fig. 5). The chosen wavelength sets give good differentiation between cyts c_1 and c_2, with reasonable error.

Tables 2 and 3 give coefficients that can be used to determine the kinetics of *all* 5 individual electron carriers using new sets of wavelengths. Only the smallest sets that give good differentiation between cyts c_1 and c_2, with reasonable error, are shown here. These tables provide the simplest sets that take into account possible spectral interference between all individual components.

These tables can be used to determine kinetics of individual components similar to that given by Eq. (6), using simple spreadsheet software.

An obvious caveat is that wavelengths sets providing maximal difference between components may often involve measurements on the steep part of an absorbance curve. It is therefore essential that the monochromator calibration and bandwidth agree with the basis spectra used here to ensure that the coefficients of Tables 1–3 are appropriate.

4.4. Comparison of the kinetics of individual components obtained by LS and DW approaches

It is important to recognize that the number of wavelengths, the choice of wavelengths and how they are used (LS vs. DW) are all important for proper deconvolution. The main difference between the DW and LS approaches is the use of the balance Eqs. (1) and (2) in the LS approach and its omission in the DW approach.

Table 4 compares the results of LS and DW analyses and summarizes conditions where the DW method is most prone to error. Substantial differences are seen in the kinetics of individual components measured by DW and LS approaches. Inaccuracies in previous determinations of the kinetics of individual components call for reevaluation of some quantitative properties

Table 4
Summary of differences in the kinetics of individual components between LS and DW approaches

Component	LS deconvolution in comparison to DW approach
b_H heme	Generally, a good correspondence between LS and DW approaches is observed, but significant differences between LS and DW kinetics can be observed in experiments where changes of cyt b_H are small. These include the following frequently employed conditions: (a) During the initial lag and early onset kinetics of cyt b_H reduction, the concentration changes are small, and contributions from cyt c_{tot}, P870 and residual electrochromic changes can significantly modify the measured kinetics [11]. (b) When b_H is reduced by multiple flashes in the presence of antimycin, the first flash induces almost complete cyt b_H reduction, and subsequent flashes cause only small changes of cyt b_H. Therefore, the relative contribution from uncompensated components increases, leading to a greater distortion of the cyt b_H kinetics in the second and later flashes in the DW approach [11]; (c) The reduction of cyt b_H *via* the Qi site in the presence of inhibitors of the Qo site is usually small at pH <8 [28,29], and distortion due to input from other components can be significant.
b_L heme	Cyt b_L is the most difficult component to measure by both LS and DW approaches, because its reduction is small in most experiments. Correspondence is generally poor but can be improved by additional *ad hoc* compensation in the DW approach for components other than cyt b_H [11]. LS analysis provides significant improvement in the measurement of b_L heme [11].
cyt c_1	If the published wavelength pairs [7] are used, the kinetics of flash-induced cyt c_1 oxidation determined by the LS approach are slower than those determined by the DW approach for the same data set (halftime ~235 μs compared to ~120 μs in the presence of antimycin). In addition, the delay of ~50 μs in the kinetics of cyt c_1 oxidation, seen using the LS approach, is masked in DW approach [10]. The correspondence between LS and DW for fast time scales is good if, in the latter, care is taken to match reference spectra and wavelengths calibration. However, even in this case a considerable difference between LS and DW approaches is observed for longer times (>0.5 ms), due to interference from cyt *b* in DW measurements. LS analysis therefore provides a significant improvement in measurement of cyt c_1 both for fast and slow time scales [10].
cyt c_2	LS and DW approaches show generally good correspondence for short times [10]. A considerable difference at longer times (>0.5 ms) is due to interference from cyt *b* in DW measurements, as for cyt c_1. LS analysis provides significant improvement in measurement of cyt c_2.
P870	Good correspondence is usually observed between LS and DW approaches [11]. Under unusual circumstances, such as in the case of cyt c_2 superproducing mutant, the difference between DW and LS can be significant.
cyt c_{tot}	Good correspondence between DW and LS analyses is usually observed [10,11]. Some differences between LS and DW analyses can be seen for times >0.5 ms due to the interference with cyt *b* in the DW approach.

of the bc_1 complex (halftimes, amplitudes, delays, etc.), especially under conditions when changes of the species of interest are relatively small and other components, with weaker absorbance at the same wavelengths used, can contribute significantly. These are conditions that will often be necessary for further exploration of the mechanism of the bc_1 complex.

The DW approach has been the de facto method of spectral and kinetic analysis in the development and testing of the Q-cycle mechanism of the bc_1 complex. However, the DW approach can significantly distort the kinetics of individual components due to its neglect of absorbance changes of other components present in the system and its poor capability to separate absorbance changes of components with overlapping spectral bands [10,11]. This raises the question whether the LS analysis undermines any of the previous evidence in favor of the Q-cycle. Detailed comparison of the kinetics of individual components obtained by DW and LS analyses has been provided previously for cyt *b* hemes [11] and for cyt c_1 [10]. Both the full LS analysis described earlier [10,11], and the simplified LS analysis presented here, indicate that the previously determined kinetics of individual components are in qualitative correspondence with the expectations of the Q-cycle. We conclude from this that none of the basic features of Q-cycle mechanism are called into question by the improved kinetic resolution provided by the LS approach.

However, the comparison of Table 4 emphasizes the need for better resolution of individual components to make further progress in understanding the function of the cyt bc_1 complex. An additional need in the chromatophore system is to incorporate corrections for electrochromic changes from carotenoids and to allow an extension of the LS analysis to coupled conditions, when these non-linear changes in the light-harvesting pigments further complicate the spectrum [18,29].

4.5. Applicability of the approach to the analysis of kinetics of bc_1 complex from different sources

To take into account overlapping of absorbance bands we have used a standard LS approach (sometimes called "classical least squares"). In the present paper, we have explored a simplified LS analysis based on small sets of wavelengths. The application depends on knowledge of the difference spectra of the individual components, in this case the spectra of P870, b_L, b_H, cyt c_2 and cyt c_1 in *Rb. sphaeroides.* In other bc_1 complexes, the spectra of b_L and b_H hemes will show variation from those measured in this work. Use of the simplified LS analysis in other organisms will require acquisition of similar reference spectra, for example in applications using *Rb. capsulatus*, also frequently employed in bioenergetics studies [30,31], in mitochondrial complexes from different species, and in oxygenic photosynthesis, where the *b6f* complex has a similar mechanism but different component spectra.

Without resolution of the kinetics of the separate components of the bc_1 complex, especially the *b*-hemes, detailed mechanistic analysis is, obviously, not possible. For the purple bacteria, the spectral separation of bc_1 components has been attempted in considerable detail using different protocols, generally with significant success. Even here, however, the simplified LS analysis presents a significant improvement over the DW method. In other systems, most notably the mitochondrial bc_1 complexes, the methods of spectral separation are significantly less evolved and the LS approach should provide a substantial advantage, well worth the effort of developing the high quality of

component spectra needed to apply it. The simplified LS approach based on small numbers of carefully chosen wavelengths could obviously be applied to the study other complex cytochrome systems.

Acknowledgements

We thank Jon Larson for major contributions to instrumentation.

This work was supported by National Institute of Health grants GM 53508 (to C.A.W. and V.P.S.) and GM 35438 (to A.R.C.).

References

[1] A.R. Crofts, C.A. Wraight, The electrochemical domain of photosynthesis, Biochim. Biophys. Acta 726 (1983) 149–185.
[2] W.A. Cramer, D.B. Knaff, Energy Transduction in Biological Membranes, Springer-Verlag, New York, 1990.
[3] E.A. Berry, M. Guergova-Kuras, L.S. Huang, A.R. Crofts, Structure and function of cytochrome *bc* complexes, Annu. Rev. Biochem 69 (2000) 1005–1075.
[4] B.L. Trumpower, A concerted, alternating sites mechanism of ubiquinol oxidation by the dimeric cytochrome bc_1 complex, Biochim. Biophys. Acta 1555 (2002) 166–173.
[5] A.R. Crofts, Proton-coupled electron transfer at the Qo-site of the bc_1 complex controls the rate of ubihydroquinone oxidation, Biochim. Biophys. Acta 1655 (2004) 77–92.
[6] J.R. Bowyer, S.W. Meinhardt, G.V. Tierney, A.R. Crofts, Resolved difference spectra of redox centers involved in photosynthetic electron flow in *Rhodopseudomonas capsulata* and *Rps. sphaeroides*, Biochim. Biophys. Acta 635 (1981) 167–186.
[7] S.W. Meinhardt, A.R. Crofts, Kinetic and thermodynamic resolution of cytochrome c_1 and cytochrome c_2 from *Rps. sphaeroides*, FEBS Lett. 149 (1982) 223–227.
[8] A.R. Crofts, S.W. Meinhardt, K.R. Jones, M. Snozzi, The role of the quinone pool in the cyclic electron-transfer chain on *Rhodopseudomonas sphaeroides* — a modified Q-cycle mechanism, Biochim. Biophys. Acta 723 (1983) 202–218.
[9] S.W. Meinhardt, A.R. Crofts, The role of cytochrome b566 in the electron transfer chain of *Rps. sphaeroides*, Biochim. Biophys. Acta 723 (1983) 219–230.
[10] V.P. Shinkarev, A.R. Crofts, C.A. Wraight, In situ kinetics of cytochromes c_1 and c_2, Biochemistry (in press).
[11] V.P. Shinkarev, A.R. Crofts, C.A. Wraight, Spectral analysis of the bc_1 complex components in situ: beyond the traditional difference approach, Biochim. Biophys. Acta 1757 (2006) 67–77.
[12] P.R. Rich, P. Heathcote, D.A. Moss, Kinetic-studies of electron-transfer in a hybrid system constructed from the cytochrome *bf* complex and photosystem I, Biochim. Biophys. Acta 892 (1987) 138–151.
[13] F.A. de Wolf, K. Krab, R.W. Visschers, J.H. de Waard, R. Kraayenhof, Studies on well-coupled Photosystem 1-enriched subchloroplast vesicles — characteristics and reinterpretation of single- turnover cyclic electron transfer, Biochim. Biophys. Acta 936 (1988) 487–503.
[14] S.W. Meinhardt, Electron Transfer Reactions of the Ubiquinol: Cytochrome c_2 Oxidoreductase of *Rhodopseudomonas sphaeroides*, University of Illinois at Urbana-Champaign, Urbana, IL, 1983.
[15] V.P. Shinkarev, S.M. Dracheva, A.L. Drachev, The thermodynamic characteristic of four-heme cytochrome c in *Rhodopseudomonas viridis* reaction centers, as derived from a quantitative analysis of the difference absorption spectra in alpha domain, FEBS Lett. 261 (1990) 11–13.
[16] K. Konishi, S.R. Vandoren, D.M. Kramer, A.R. Crofts, R.B. Gennis, Preparation and characterization of the water-soluble heme-binding domain of cytochrome c_1 from the *Rhodobacter sphaeroides* bc_1 complex, J. Biol. Chem. 266 (1991) 14270–14276.
[17] L.A. Drachev, B.S. Kaurov, M.D. Mamedov, A.J. Mulkidjanian, A.J. Semenov, V.P. Shinkarev, V.P. Skulachev, M.I. Verkhovsky, Flash-induced electrogenic events in the photosynthetic reaction center and *bc* complex of *Rhodobacter sphaeroides* chromatophores, Biochim. Biophys. Acta 973 (1989) 189–197.
[18] V.P. Shinkarev, A.R. Crofts, C.A. Wraight, The electric field generated by photosynthetic reaction center induces rapid reversed electron transfer in the bc_1 complex, Biochemistry 40 (2001) 12584–12590.
[19] J.C. Sternberg, H.S. Stillo, R.H. Schwendeman, Spectrophotometric analysis of multicomponent systems using the least squares method in matrix form. The ergosterol irradiation system, Anal. Chem. 32 (1960) 84–90.
[20] D.M. Bates, D.G. Watts, Nonlinear Regression Analysis and its Applications, John Wiley & Sons Inc, New York, 1988.
[21] N.R. Draper, H. Smith, Applied Regression Analysis, John Wiley & Sons Inc, New York, 1998.
[22] R.A. Johnson, D.W. Wichern, Applied Multivariate Statistical Analysis, 4th ed., Prentice Hall, Upper Saddle River, NJ, 1998.
[23] G.H. Golub, C.F. Van Loan, Matrix Computations, 3rd ed., The John Hopkins University Press, Baltimore, 1996.
[24] J.D. Hoffman, Numerical Methods for Engineers and Scientists, 2nd ed., Marcel Dekker, Inc, New York, 2001.
[25] C.D. Meyer, Matrix Analysis and Applied Linear Algebra, SIAM, Philadelphia, 2000.
[26] S.J. Leon, Linear Algebra with Applications, 6 ed., Prentice Hall, Upper Saddle River, NJ, 2002.
[27] A.R. Crofts, V.P. Shinkarev, D.R.J. Kolling, S.J. Hong, The modified Q-cycle explains the apparent mismatch between the kinetics of reduction of cytochromes c_1 and b_H in the bc_1 complex, J. Biol. Chem. 278 (2003) 36191–36201.
[28] P.L. Dutton, K.M. Petty, S. Bonner, S.D. Morse, Cytochrome c_2 and reaction center of *Rhodopseudomonas sphaeroides* Ga membranes. Extinction coefficients, content, half-reduction potentials, kinetics and electric field alterations, Biochim. Biophys. Acta 387 (1975) 536–556.
[29] G. Venturoli, M. Virgili, B.A. Melandri, A.R. Crofts, Kinetic measurements of electron transfer in coupled chromatophores from photosynthetic bacteria: a method of correction for the electrochromic effects, FEBS Lett. 219 (1987) 477–484.
[30] A.S. Saribas, H.G. Ding, P.L. Dutton, F. Daldal, Substitutions at position 146 of cytochrome b affect drastically the properties of heme b_L and the Qo site of *Rhodobacter capsulatus* cytochrome bc_1 complex, Biochim. Biophys. Acta 1319 (1997) 99–108.
[31] A. Osyczka, C.C. Moser, F. Daldal, P.L. Dutton, Reversible redox energy coupling in electron transfer chains, Nature 427 (2004) 607–612.